communications biology

A Nature Portfolio journal

Article

https://doi.org/10.1038/s42003-025-07946-8

Extracellular osmolarity regulates osteoblast migration through the TRPV4-Rho/ROCK signaling

Yijie Li[1,3], Yanyan Yang[1,3], Xiaohuan Wang[1,3] ✉, Long Li[2] ✉ & Mouwang Zhou[1] ✉

For precise bone formation, osteoblasts need to accurately migrate to specific sites guided by various biochemical and mechanical cues. During this migration, fluctuations in extracellular osmolarity may arise from shifts in the surrounding fluid environment. However, as a main regulator of cell morphology and function, whether the extracellular osmolarity change may affect osteoblast migration remains unclear. Here, we provide evidence showing that changes in extracellular osmolarity significantly impact osteoblast migration, with a hypotonic environment enhancing it while a hypertonic environment inhibiting it. Further, our findings reveal that a hypotonic treatment increases intracellular pressure, activating the Transient Receptor Potential Vanilloid 4 (TRPV4) channel. This activation of TRPV4 modulates stress fibers, focal adhesions (FAs), and cell polarity through the Rho/ROCK signaling pathway, ultimately impacting osteoblast migration. Our findings provide valuable insights into the significant influence of extracellular osmolarity on osteoblast migration, which has potential implications for enhancing our understanding of bone remodeling.

Osteoblasts, originating from mesenchymal stem cells, play essential roles in maintaining bone homeostasis[1]. They are crucial for synthesizing and mineralizing the bone matrix, key processes in bone formation, remodeling, and repair. These specialized cells help maintain skeletal integrity and facilitate the regeneration of bone tissue, whether in response to injury or as part of normal physiological turnover[2]. To participate in bone formation, osteoprogenitor cells need to first migrate to the action region. Thus, osteoblast migration constitutes an incipient step in bone formation, and increasing attention has been paid to enhancing osteoblast migration to improve the therapeutic efficacy of bone diseases[3,4].

Bone is a dynamic tissue that constantly undergoes bone damage and remodeling throughout its lifespan[5]. Wolff's law indicates that bone adapts its structure in response to mechanical loading, implying that mechanical signals are crucial regulators of bone growth, reconstruction, and metabolism[6,7]. The mechanical environment, including factors like fluid shear stress, stretch stress, substrate stiffness, and substrate topology, has a significant impact on bone cell migration. Gao et al. demonstrated that osteoclast precursor cells can detect fluid shear stress and migrate toward areas of lower stress through the regulation of the calcium signaling pathway[8]. Additionally, MC3T3-E1 cells were observed to present higher migration speed on patterned surfaces compared to flat surfaces[9]. Further, cyclic mechanical stretching was also reported to improve the migration of MC3T3-E1 cells[10].

Cell migration is a fundamental process in biology that underpins crucial events in tissue formation, repair, and regeneration[11]. Understanding the intricate mechanisms underlying cell migration is essential for developing therapies for diseases characterized by aberrant cell movements, such as osteoporosis and cancer[12]. To initiate migration, cells first need to polarize and extend protrusions in the migration direction. The establishment of cell polarity is a fascinating symmetry-breaking process controlled by various factors including the extracellular matrix (ECM), Rho GTPase, and the cytoskeleton in response to extracellular chemical signals[11,13]. Recent researches indicate that mechanical factors also play a role in establishing and maintaining cell polarity. Houk et al. demonstrated that membrane tension is the dominant factor in maintaining cell polarity during neutrophil migration[14]. Substrate rigidity can alter the front-rear polarity of migrating cells, directing them to move toward stiffer environments[15]. Fibroblasts cultured on soft substrates submitted to cyclic stretch will reorient their stress fibers either parallel or perpendicular to the stress direction[16]. Thus, the generation and maintenance of cell polarity to guide cell migration can be regulated by both biochemical and mechanical signals[17].

[1]Department of Rehabilitation Medicine, Peking University Third Hospital, 49 North Garden Road, Beijing, 100191, China. [2]State Key Laboratory of Nonlinear Mechanics and Beijing Key Laboratory of Engineered Construction and Mechanobiology, Institute of Mechanics, Chinese Academy of Sciences, Beijing, 100190, China. [3]These authors contributed equally: Yijie Li, Yanyan Yang, Xiaohuan Wang. ✉e-mail: wangxh0808@126.com; lilong@lnm.imech.ac.cn; zhoumwpku@163.com

During osteoblast migration, the extracellular fluid environment may vary as they move from the bone marrow to the destination. Additionally, the flow of interstitial fluid when the bone experiences stress, may also affect the extracellular fluid environment[18]. A key factor related to the extracellular fluid environment is osmolarity, which plays a crucial role in regulating cell morphology and function. In a hypotonic environment, the water inflow increases intracellular pressure, causing the cell to swell. This can affect processes such as proliferation, differentiation, migration, and signal transduction. In a hypertonic environment, cells shrink, which can interfere with functions like cytoskeletal integrity, adhesion, and metabolism. Both conditions significantly impact cell behavior and are essential for processes like tissue repair, development, and immune responses[19,20]. Petrie et al. revealed that cells utilize lamellipodia for migration under low intracellular pressure conditions, whereas high intracellular pressure prompts the formation of lobopodia to facilitate migration[21]. Moreover, cell migration in confined microenvironments is driven by the regulation of water permeation through extracellular osmolarity[22]. Nevertheless, the impact of extracellular osmolarity on the morphology and migration of osteoblasts in bone has not yet been fully investigated and remains uncertain.

In this study, we employed the MC3T3-E1 cell line, a commonly utilized osteoblast model, to investigate the influence of extracellular osmolarity on osteoblast migration. Our research findings present compelling evidence for the significant involvement of extracellular osmolarity in governing osteoblast migration. We specifically demonstrated that osteoblasts perceive alterations in extracellular osmolarity through the TRPV4 channel. This channel, in turn, governs stress fibers, FAs, and cell polarity by regulating the Rho/ROCK signaling pathway, leading to a direct impact on osteoblast migration.

Results

Extracellular osmolarity affects osteoblast migration

To explore the effects of extracellular osmolarity on osteoblast migration, we exposed adherent MC3T3-E1 cells labeled with Hoechst 33342 to media with varying osmolarities. The migration of osteoblasts was then monitored using time-lapse imaging in a live cell workstation. Analysis of the osteoblast migration paths over 12 h showed that osteoblasts traveled significantly longer distances in the hypotonic medium compared to the isotonic medium, while their trajectories were much shorter in the hypertonic medium (Fig. 1a). Analysis of migration speeds revealed that osteoblasts exhibited the highest average migration speed in the hypotonic medium, reaching 0.09 μm per minute. In the isotonic medium, the average migration speed was ~0.06 μm per minute, while in the hypertonic medium, the average speed was around 0.05 μm per minute (Fig. 1b). To further confirm the effect of extracellular osmolarity on osteoblast migration, we conducted

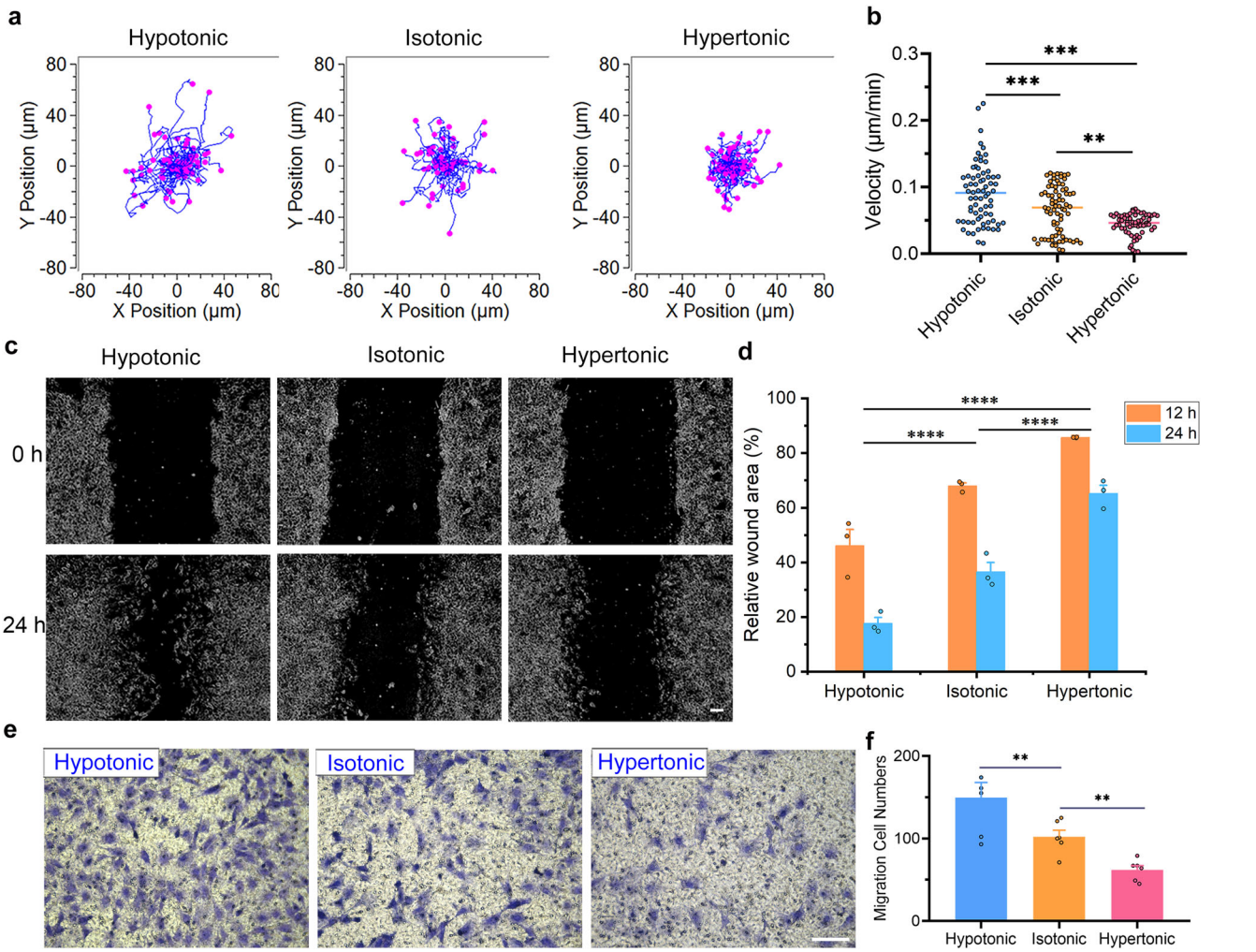

Fig. 1 | Extracellular osmolarity affects osteoblast migration. a, **b** Trajectories (**a**) and statistical migration speed (**b**) of MC3T3-E1 cells in media with different osmolarities over 12 h ($n > 60$). **c**, **d** Screenshot of wound-healing assay at 0 and 24 h (**c**) and statistical analysis of wound-healing speed (**d**) in media with different osmolarities ($n = 3$). **e**, **f** Representative images of transwell experiments (**e**) and statistical results of migration cell numbers of MC3T3-E1 cells (**f**) in media with different osmolarities over 12 h ($n = 6$). $^{**}P < 0.01$, $^{***}P < 0.001$, $^{****}P < 0.0001$ as assessed using one-way ANOVA followed by Tukey's test (**b**, **f**) and two-way ANOVA followed by Tukey's test (**d**). All data were reported as the mean ± standard error of the mean (SEM). Scale bars: 100 μm.

wound healing experiments to evaluate the collective migration and wound closure capabilities of osteoblasts in media with varying osmolarities. The results showed that hypotonic conditions accelerated the healing process, while hypertonic environments significantly slowed it down (Fig. 1c, d). Additionally, we utilized the transwell assay to evaluate the chemotactic migration of osteoblasts in response to changes in extracellular osmolarity by adjusting the osmolarities in the wells of the plate. We observed an increased number of cells migrating through the pores toward the hypotonic environment (Fig. 1e, f), suggesting that extracellular osmolarity may play a role in directing osteoblast migration. Apoptosis analysis indicated no significant differences in cell apoptosis rates across the different osmolarities within 24 h, highlighting the impact of extracellular osmolarity on osteoblast migration (Supplementary Fig. 1). Overall, these findings emphasize the pivotal role of extracellular osmolarity as a critical regulator in osteoblast migration, with hypotonic conditions promoting migration while hypertonic environments inhibiting it.

Extracellular osmolarity regulates focal adhesions, stress fibers, and the polarity of osteoblast

Cell migration relies heavily on the interplay between cells and their surrounding extracellular matrix[23]. Central to this process is the focal adhesion (FA) that connects the cytoskeleton to the extracellular matrix, as well as the overall structure of the cytoskeleton[11,24]. Building on this knowledge, we proposed that fluctuations in extracellular osmolarity can impact osteoblast migration by influencing the stability and organization of FAs and the cytoskeleton. To investigate the influence of extracellular osmolarity on the cytoskeleton structure, we labeled osteoblasts with phalloidin after exposing them to media with varying osmolarities for 12 h. The results showed that the hypotonic medium favored the formation of stress fibers while the hypertonic medium was adverse to the formation of stress fibers (Fig. 2a–c). Furthermore, we conducted a time-gradient analysis to observe cytoskeletal changes following osmotic pressure stimuli. Our findings indicate that the cytoskeleton responds rapidly to these stimuli, with the most pronounced differences between groups observed at the 3-h mark. Cells in the hypotonic medium groups displayed the most organized and polarized cytoskeletal structures. However, these differences gradually diminished over time and were significantly reduced by the 24-h mark (Supplementary Fig. 2). The results demonstrate that cells adapt to and mitigate the initial changes in extracellular osmolarity. Additionally, staining with paxillin revealed that extracellular osmolarity influenced the formation of FAs. Notably, the number of FAs greatly increased in the hypotonic medium and decreased in the hypertonic medium (Fig. 2a–c and Supplementary Fig. 3).

FAs and the organization of stress fibers are often associated with the generation of traction forces, which are essential for establishing cell polarity to facilitate cell migration[25]. To examine the impact of extracellular osmolarity on osteoblast polarity, we initially analyzed the aspect ratio of osteoblasts to assess polarity changes. Our results showed that osteoblasts presented an average aspect ratio of about 2.7 in the isotonic medium. This ratio increased to ~5.4 in the hypotonic medium and decreased to around 2.0 in the hypertonic medium (Fig. 2d). Further, we quantified the orientation of stress fibers (Fig. 2e). In the hypotonic medium, stress fibers tended to align parallel to the long axis of the osteoblasts. The angles between the stress fibers and the long axis of the osteoblasts were primarily distributed in the range of 0–22.5 and 157.5–180 degrees. As extracellular osmolarity increased from hypotonic to hypertonic, the distribution of these angles gradually spread out (Fig. 2f–h). Collectively, these findings indicate that extracellular osmolarity plays a significant role in the formation of FAs, stress fibers, and the development of cell polarity.

Osteoblast senses extracellular osmolarity change through the TRPV4 channel

We have demonstrated that extracellular osmolarity plays a significant role in regulating osteoblast migration. Yet, a key question remains: how do osteoblasts detect changes in extracellular osmolarity and subsequently adjust cytoskeletal structure and cell polarity to modulate migration? Since the cell membrane is semipermeable, changes in the extracellular osmolarity will cause water flux through the membrane, leading to intracellular pressure change. Intracellular pressure governs the membrane stretching that affects the stretch-activated channels, which mainly respond to the tension change and transduce the mechanical signals to biological signals[19,26]. To test the effects of extracellular osmolarity change on intracellular pressure, we measured the intracellular pressure of MC3T3-E1 cells in media with different osmolarities using the servo-null method within a 15- to 30-min timeframe[21]. In the isotonic medium (300 mOsm), the average intracellular pressure of osteoblasts was measured at ~455 Pa. Contrastingly, in the hypotonic medium (240 mOsm), the average intracellular pressure increased to around 685 Pa and decreased to about 245 Pa in the hypertonic medium (360 mOsm) (Fig. 3a). These findings suggest that modulating extracellular osmolarity significantly affects intracellular pressure.

The primary impact of elevated intracellular pressure on cells is the escalation of tension in the cell membrane. This rise in tension can lead to stretching, potentially activating calcium channels responsible for transducing the force into biochemical signals[26]. Calcium ion concentration significantly influences bone metabolism and cell signaling. The flow of calcium ions is considered a key signal enabling bone tissue to adapt to mechanical stimuli[27]. Additionally, changes in intracellular calcium concentration correlate directly with the intensity of mechanical stimuli; higher intensity stimuli produce more pronounced calcium responses, as evidenced by an increase in the number of calcium peaks, higher amplitudes, and faster response rates[28]. Previous research has suggested that the cation channel TRPV4 responds to membrane stretching[29,30] and TRPV4 is a critical regulator of cell volume in response to osmolarity change[31]. Thus, it is reasonable to propose that osteoblasts utilize the TRPV4 channel for detecting alterations in extracellular osmolarity. To validate this hypothesis, we examined the calcium ion concentration in MC3T3-E1 cells during hypotonic shock. The findings demonstrated a rapid increase in cellular calcium concentration, peaking at approximately 20 s before gradually declining (Fig. 3b–e). Additionally, inhibition of the TRPV4 channel with the TRPV4 antagonist HC067047 (HC)[32] significantly suppressed the observed increase in calcium concentration (Fig. 3d–f). Taken together, these results support that osteoblasts primarily respond to changes in extracellular osmolarity through the TRPV4 channel.

TRPV4 plays a critical role in regulating osteoblast migration

To investigate the impact of TRPV4 on osteoblast migration, we conducted experiments to inhibit the TRPV4 channel and assessed cell migration through live cell tracking, wound healing, and transwell assays. In all of these experiments, the inhibition of TRPV4 resulted in a significant reduction in osteoblast migration (Fig. 4a–c). Moreover, we sought to explore the influence of TRPV4 on the cellular cytoskeleton and FAs. To achieve this, we utilized HC to inhibit TRPV4 in conjunction with hypotonic treatment, and GSK1016790A (GSK)[32] to activate TRPV4 alongside hypertonic treatment. Our results indicated that when TRPV4 inhibition was combined with hypotonic treatment, there was a noticeable decline in stress fiber formation and a decrease in the number of FAs when compared to hypotonic treatment alone (Figs. 2a, 4d and Supplementary Fig. 3). On the contrary, when TRPV4 was activated alongside hypertonic treatment, it stimulated stress fiber formation, resulting in a substantial increase in the number of FAs compared to hypertonic treatment alone (Figs. 2c, 4e and Fig. S3). We also examined the effect of TRPV4 on osteoblast polarity. Analysis of the aspect ratio revealed that inhibiting TRPV4 in the hypotonic medium decreased the average aspect ratio from about 5.4 to 3.7, while activating TRPV4 in the hypertonic medium slightly increased the aspect ratio from about 2.0 to 2.2 (Fig. 4f). Additionally, statistical analysis of stress fiber orientation revealed that inhibiting TRPV4 in the hypotonic medium dispersed stress fiber alignment, while activating TRPV4 channels in the hypertonic medium caused stress fibers to align closer to the long axis of the osteoblasts (Figs. 2f, h, 4g, h). Together, these results indicate that TRPV4 plays a crucial role in osteoblast migration.

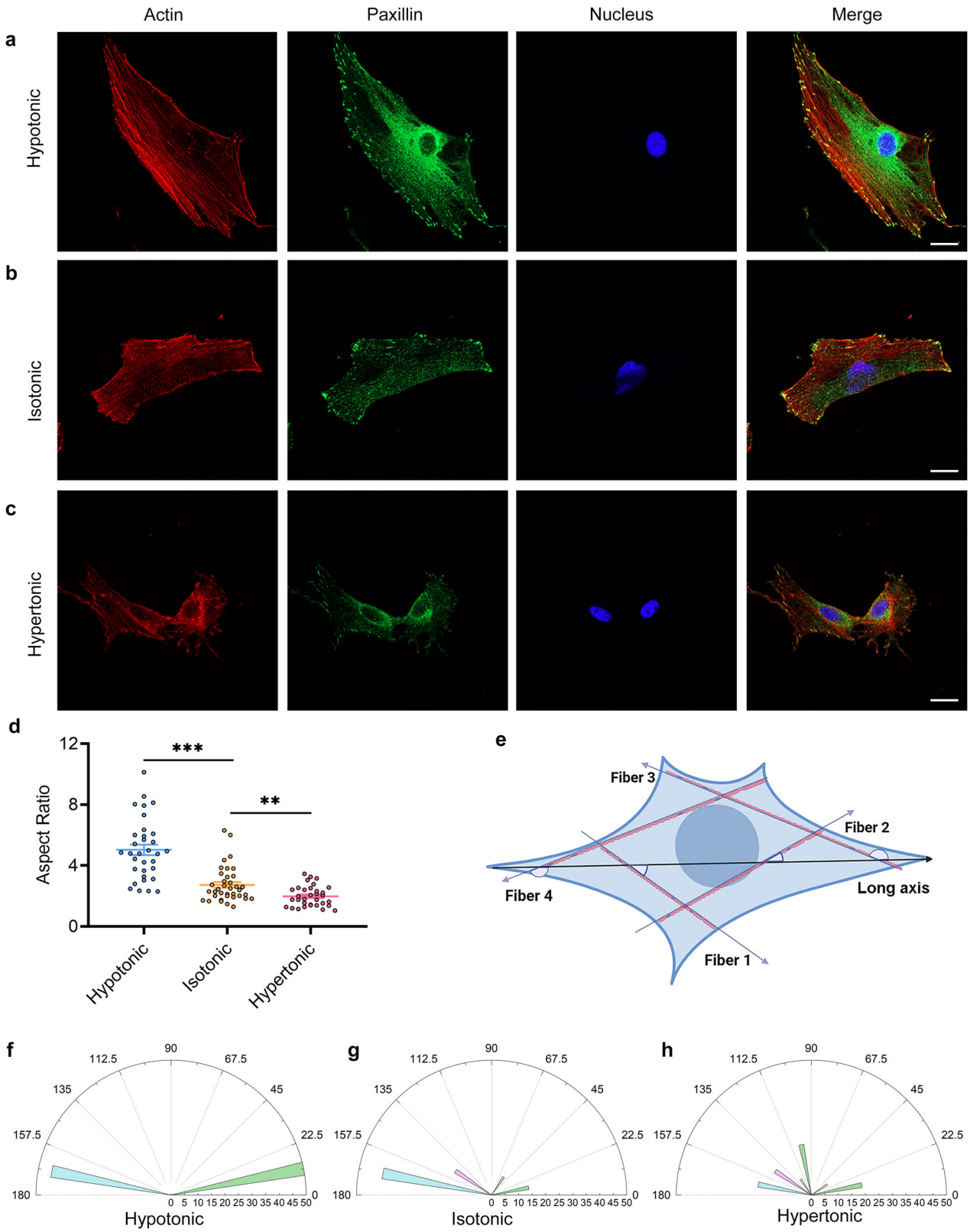

Fig. 2 | Extracellular osmolarity affects the development of cell polarity. **a**–**c** Immunofluorescence staining of MC3T3-E1 cells in media with different osmolarities. **d** Aspect ratios of MC3T3-E1 cells in media with different osmolarities ($n > 30$). **e** Schematic illustrating the method of measuring stress fiber orientation. Fibers 1–4, respectively, exhibit fiber orientation measurements that deviate from the long axis of the cell. **f**–**h** The wind rose diagrams of stress fiber direction in cells cultured in media with different osmolarities (Stress fibers included in the analysis were obtained from five different cells in each group). $^{**}P < 0.01$, $^{***}P < 0.001$ as assessed using one-way ANOVA followed by Tukey's test (**d**). Data in (**d**) are reported as mean ± SEM. Scale bars: 20 μm (**a**–**c**).

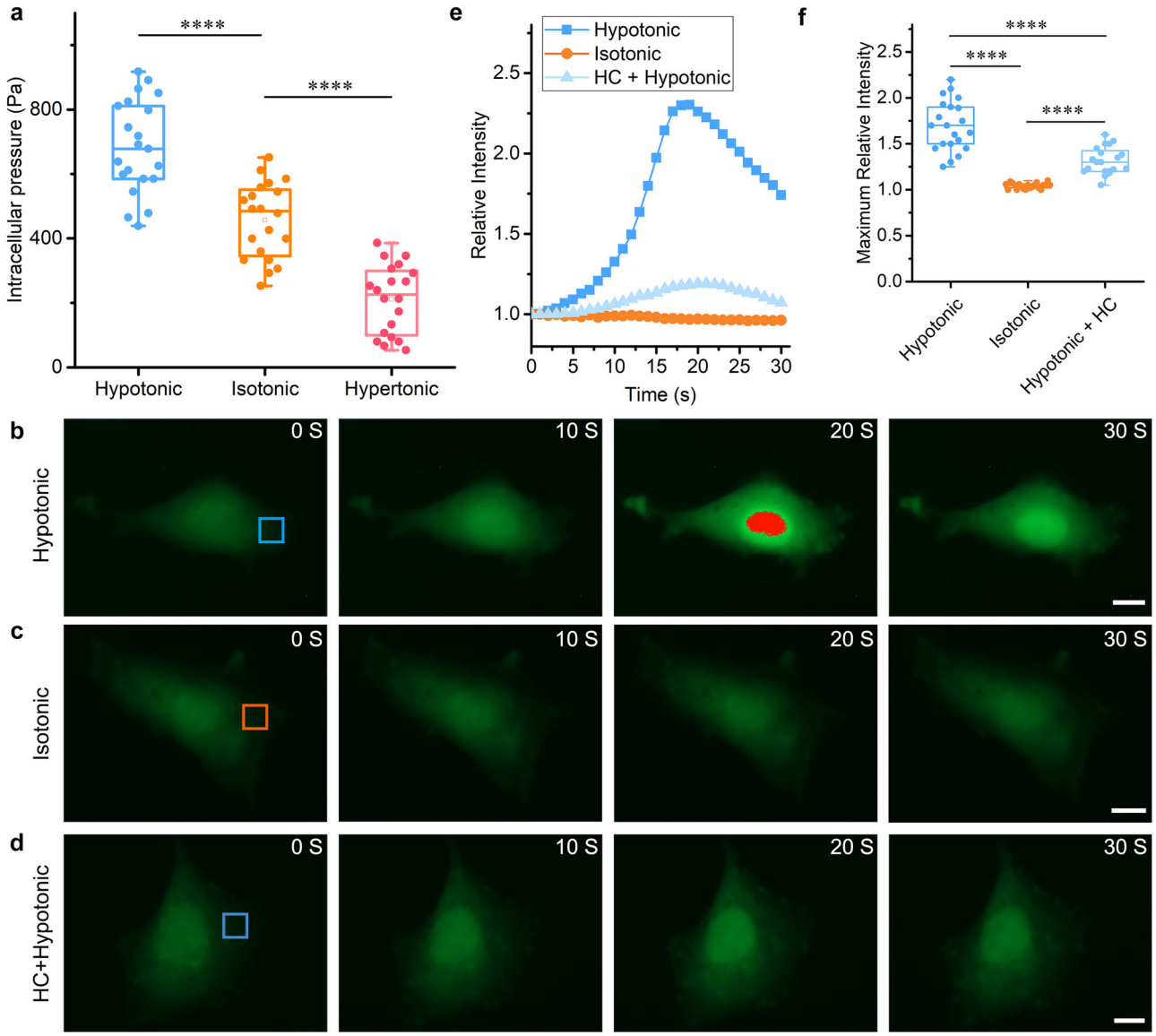

Fig. 3 | Osteoblast responds to hypotonic shock through the TRPV4 channel. **a** Measured intracellular pressure of MC3T3-E1 cells in media with different osmolarities ($n > 20$). **b–d** Screenshots illustrating the variation in calcium ion fluorescence intensity upon hypotonic shock (**b**), in isotonic medium (**c**), and upon hypotonic shock with TRPV4 inhibition (**d**). **e**) Relative fluorescence intensity of calcium ion corresponding to experiments (**b–d**). The measured areas are indicated with color boxes. (**f**) Statistical results of maximum relative calcium fluorescence intensity upon hypotonic shock with or without TRPV4 inhibition ($n > 20$). The relative calcium fluorescence intensity was calculated by normalizing the fluorescence intensity to the value of 0 s. $^{****}P < 0.0001$ as assessed using one-way ANOVA followed by Tukey's test (**a**) and unpaired *t*-test (**f**). Data in (**f**) are presented as the mean ± SEM. Scale bars: 20 μm.

The Rho/ROCK signaling plays a critical role in osteoblast migration and polarity

To decode how extracellular osmolarity influences osteoblast migration, we specifically focused our analysis on the Rho/ROCK signaling cascade due to its pivotal role in regulating actin dynamics and FA formation[33]. Moreover, studies have shown that the Rho/ROCK signaling pathway is closely linked with TRPV4[32,34], which underscores its relevance as a focal point in our research. We first conducted experiments to examine the impact of the Rho/ROCK signaling on osteoblast migration. To achieve this, we utilized several inhibitors specifically targeting components of the Rho/ROCK pathway. Notably, when we inhibited Rac GTPase using the NSC23766 inhibitor, Cdc42 GTPase utilizing the ML141 inhibitor, and ROCK kinase with the Y27632 inhibitor[35–37] prior to exposing the cells to hypotonic shock, the migration of osteoblasts was significantly inhibited, as demonstrated by the live cell tracking and wounding healing experiments (Fig. 5a, b). Further, we observed a significant decrease in both the formation of stress fibers and the abundance of FAs with the utilization of these Rho/ROCK inhibitors (Supplementary Figs. 3, 4). Moreover, we found a significant influence of the Rho/ROCK pathway on osteoblast polarity. Specifically, Rho or ROCK inhibition resulted in a significant decrease in the aspect ratio of osteoblasts (Fig. 5c). Further, we observed a remarkable dispersal in the alignment of stress fibers after Rho or ROCK inhibition (Fig. 5d–f). Cumulatively, the results show that the Rho/ROCK signaling pathway plays an integral role in governing the cytoskeletal dynamics and migration of osteoblasts.

Extracellular osmolarity regulates osteoblast migration through the TRPV4-Rho/ROCK signaling

After successfully demonstrating the impact of extracellular osmolarity, TRPV4 channel, and Rho/ROCK signaling on osteoblast migration and polarity development, our next objective was to

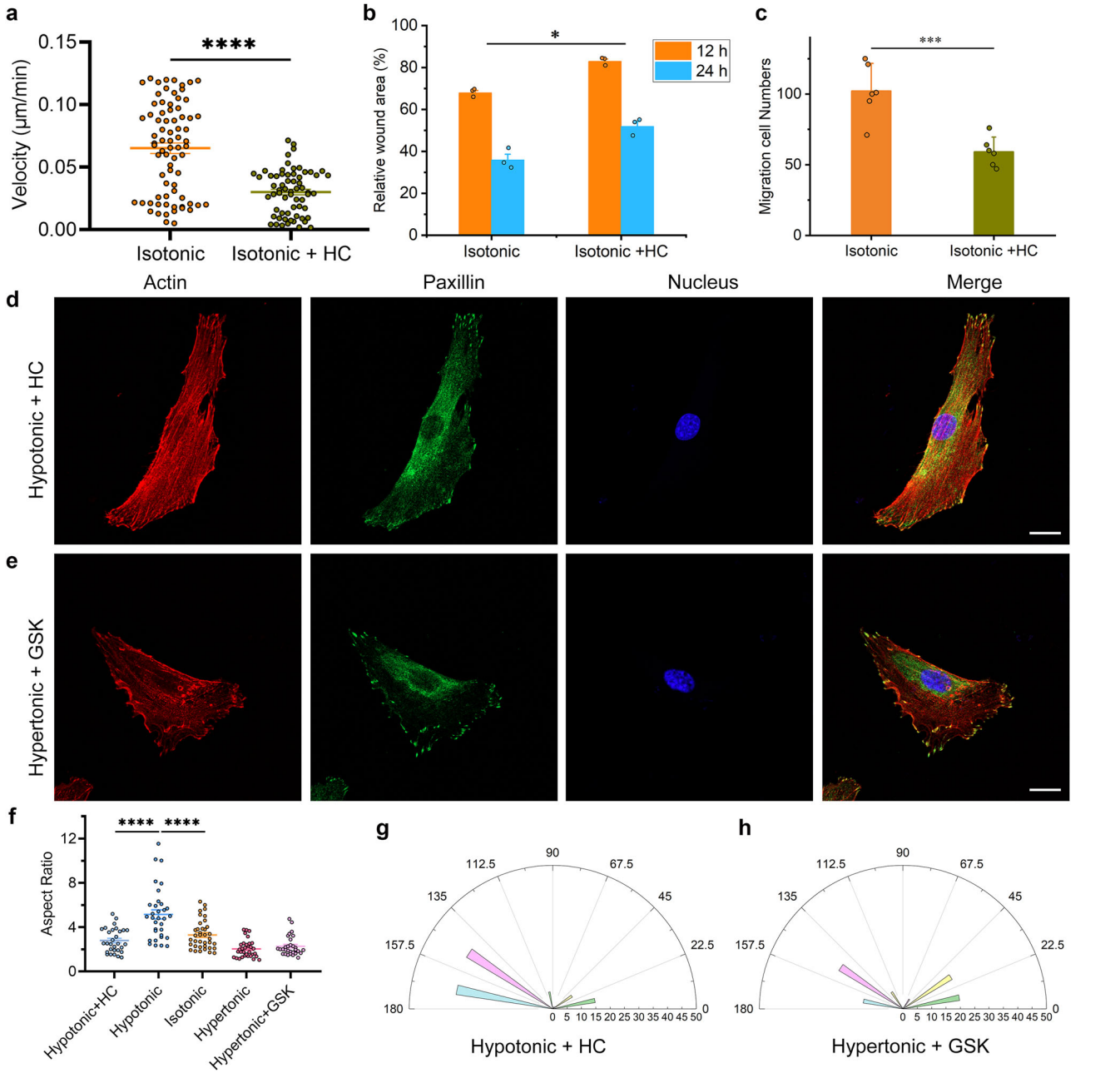

Fig. 4 | TRPV4 is pivotal in osteoblast migration and polarity development. **a**–**c** Evaluation of the osteoblast migration based on live cell tracking over 12 h ($n > 60$) (**a**), wound healing experiment over 24 h ($n = 3$) (**b**), and transwell experiments spanning 12 h ($n = 6$) (**c**). **d**, **e** Immunofluorescence staining of MC3T3-E1 cells in media with different osmolarities and HC067047 or GSK1016790A. **f** Cell aspect ratios in media with different osmolarities and HC067047 or GSK1016790A ($n > 30$). **g**, **h** The wind rose diagrams of stress fiber direction in cells cultured in media with different osmolarities and HC067047 or GSK1016790A (Stress fibers included in the analysis were obtained from five different cells). $^{*}P < 0.05$, $^{***}P < 0.001$, and $^{****}P < 0.0001$ as assessed using an unpaired *t*-test (**a**, **c**), two-way ANOVA test (**b**), and one-way ANOVA followed by Tukey's test (**f**). Data in (**a**–**c**) and (**f**) are represented as the mean ± SEM. Scale bars: 20 μm.

elucidate the interplay between these factors. To achieve this, we performed western blot and PCR experiments to quantify the expression of TRPV4 in osteoblasts exposed to varying extracellular osmolarities. Our findings from both the western blot and PCR analyses revealed that exposure to a hypotonic medium led to an increase in TRPV4 expression, whereas exposure to a hypertonic medium resulted in a decrease in TRPV4 expression levels (Fig. 6a–c).

Subsequently, we proceeded to investigate the impact of extracellular osmolarity and TRPV4 on the expression levels of Rho proteins. To elucidate this, we performed PCR analysis. Remarkably, our findings demonstrated that hypotonic treatment notably upregulated the expression levels of both CDC42 and RAC1. Conversely, a discernible decrease in the expression levels of both CDC42 and RAC1 was observed when the osteoblasts were exposed to hypertonic treatment (Fig. 6d, e). Further, when we inhibited TRPV4 along with the hypotonic treatment, a pronounced reduction in the expression of CDC42 was noted compared to pure hypotonic shock (Fig. 6d). Additionally, there was a slight decrease in the expression of RAC1. Conversely, when TRPV4 was activated in the hypertonic medium, an increase in the expression levels of both CDC42 and RAC1 was detected (Fig. 6d, e). In summary, the results indicate a regulatory relationship where extracellular osmolarity influences the expression of TRPV4. Furthermore, TRPV4 appears to function as an upstream regulator for the Rho/ROCK signaling pathway.

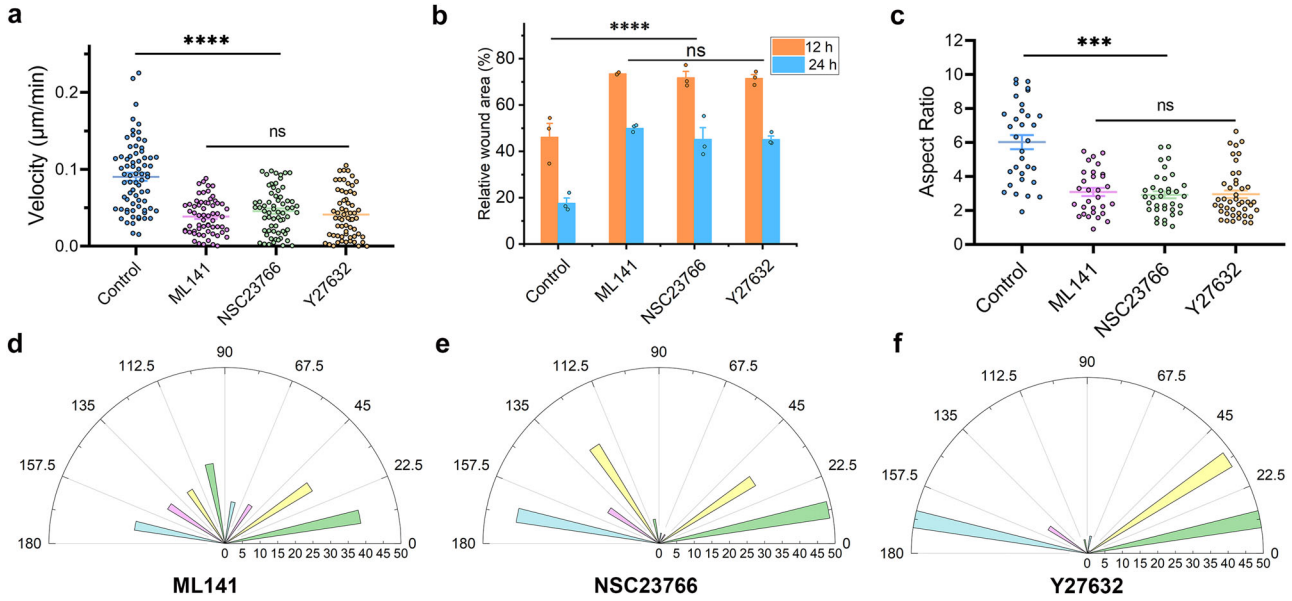

Fig. 5 | The Rho/ROCK signaling is critical in osteoblast migration and polarity. **a** Migration speed of osteoblast in the hypotonic medium under treatment of different inhibitors ($n > 60$). **b** Statistical results of wound healing experiments in hypotonic medium with different inhibitors ($n = 3$). **c** Aspect ratios of cells treated with different inhibitors ($n > 30$). **d**–**f** The wind rose diagrams of stress fiber direction in cells treated with ML141, NSC23766, or Y27632 (Stress fibers included in the analysis were obtained from five different cells in each group). ns not significant, $^{***}P < 0.001$, $^{****}P < 0.0001$ as assessed using a one-way ANOVA followed by Tukey's test (**a**, **c**) and two-way ANOVA followed by Tukey's test (**b**). Data in (**a**–**c**) are presented as mean ± SEM.

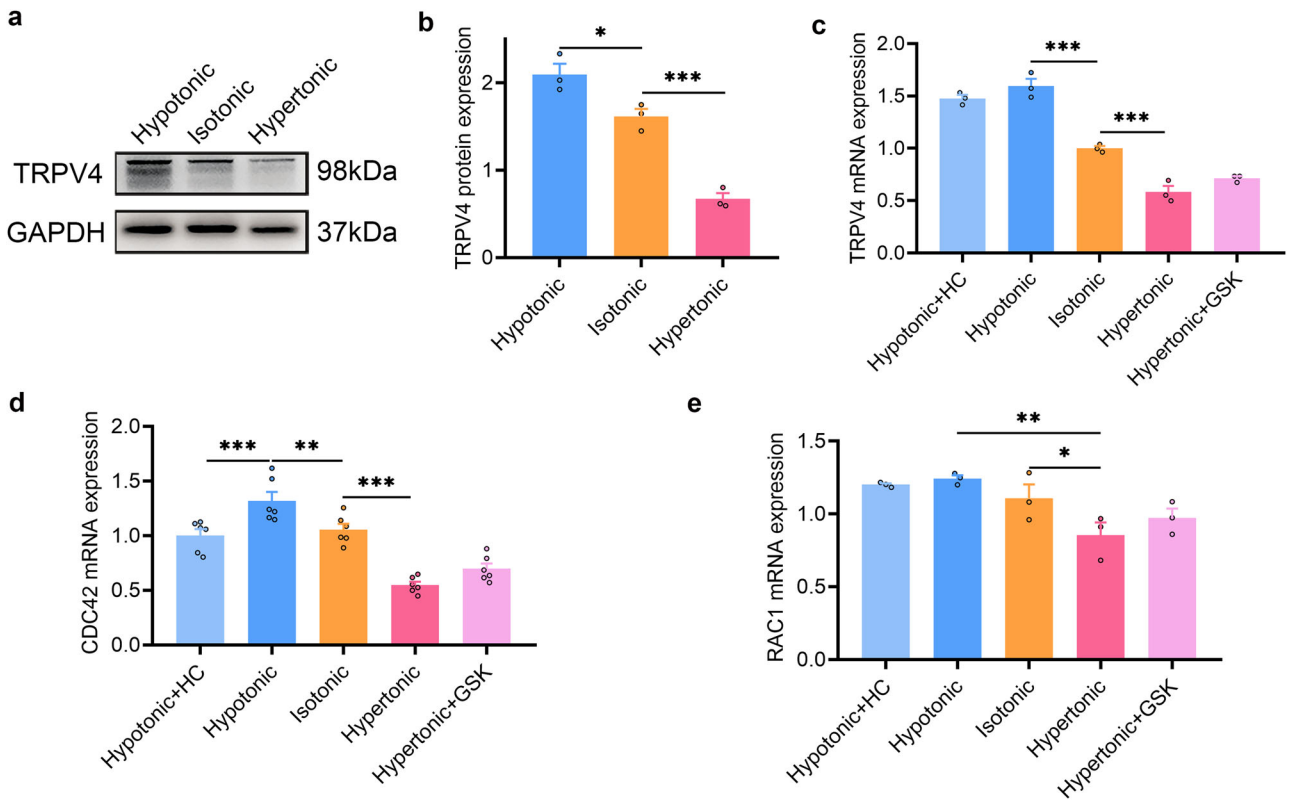

Fig. 6 | Extracellular osmolarity regulates osteoblast migration through the TRPV4-Rho/ROCK signaling. **a**, **b** Evaluation of TRPV4 protein expression based on Western blot analysis ($n = 3$). **c** Evaluation of TRPV4 gene expression through qRT-PCR ($n = 3$). GAPDH was used as a control for equal loading. **d**, **e** QRT-PCR analyzed gene expression levels of the CDC42 and RAC1 in MC3T3-E1 cells under conditions labeled on the horizontal axis (**d**, $n = 6$. **e**, $n = 3$). $^{*}P < 0.05$, $^{**}P < 0.01$, and $^{***}P < 0.001$ as assessed using a one-way ANOVA followed by Tukey's test. Data in (**b**–**e**) are presented as mean ± SEM.

Discussion

In this study, we specifically investigated the impact of extracellular osmolarity on osteoblast migration. We propose a mechanism in which extracellular osmolarity influences osteoblast migration by regulating cytoskeletal dynamics, FA formation, and cell polarity. These pathways collectively coordinate cell behavior and impact the migratory capacity of osteoblasts. Unraveling these mechanisms could provide valuable insights into the role of extracellular osmolarity in maintaining bone homeostasis and facilitating regeneration.

Previous studies have consistently demonstrated that mechanical stretch can stimulate osteoblast differentiation[38,39]. Notably, fluid shear stress has been found to exert influences on osteoblast differentiation, proliferation, and viability[40–42]. Furthermore, studies have revealed that substrate properties play a role in modulating osteoblast functionalization[43–45]. However, compared to these mechanical factors, there has been limited research on the impact of extracellular osmolarity on osteoblasts. It is important to note that extracellular osmolarity is a critical regulator closely linked to cell volume, shape, and the mechanical microenvironment[46,47]. As osteoblasts migrate from the stem cell pool to their destination, they may encounter various fluid environments, such as blood, lymph, and interstitial fluid in the bone. The osmolarities of these fluids may differ due to variations in their composition and the metabolic activity of surrounding cells[3,48]. Moreover, bone injuries typically trigger a range of changes, including inflammatory responses, fluid extravasation, edema, and alterations in cellular metabolism and necrosis. These processes can collectively contribute to changes in the osmolarity at the injury site[49,50]. Consequently, fluctuations in extracellular osmolarity are inevitable during osteoblast migration. Here, we investigated the precise effects of extracellular osmolarity on osteoblast migration and demonstrated that a hypotonic environment can promote their migration. This intriguing finding enhances our understanding of the complex factors that regulate osteoblast migration and underscores the importance of the liquid environment in bone tissue.

Mechanical loading, such as that induced by exercise, has been shown to enhance bone formation by osteoblasts and improve bone strength. However, the precise mechanisms involved in the transfer and transduction of mechanical signals are still not fully understood. The TRPV4 ion channel has been identified as playing a role in mechanotransduction[51,52]. TRPV4 interacts directly and functionally with cytoskeletal components such as actin and microtubules, adjusting cytoskeletal dynamics and calcium signaling, thereby affecting cell shape and mobility[53]. Moreover, activation of TRPV4 leads to an increase in calcium influx and modifies cytoskeletal dynamics through the regulation of key proteins like cofilin and cortactin, playing a pivotal role in cellular activities, including the metastasis of melanoma[54]. Additionally, TRPV4 controls the organization of the collagen matrix and the tension at adhesion sites in mesenchymal stem cells through calcium signaling, facilitating the mechanical adjustment of the cytoskeleton and the remodeling of the extracellular matrix[55]. In our study, we confirmed that the TRPV4 channel can detect changes in extracellular osmolarity and trigger significant changes in osteoblasts, ultimately regulating osteoblast migration. Moreover, our findings demonstrate that extracellular osmolarity regulates TRPV4 expression, uncovering a positive feedback loop whereby hypotonic treatment elevates TRPV4 levels. Consequently, TRPV4 enhances osteoblast sensitivity to fluctuations in extracellular osmolarity, ultimately facilitating the establishment of osteoblast polarity and promoting migration.

Cell polarity plays a fundamental role in guiding cell migration, as it establishes the leading edge of the migrating cell and directs its movement[23]. Cell polarization can occur through biochemical interactions such as growth factors or in response to mechanical stimuli such as substrate properties[17,56,57]. Our study reveals that extracellular osmolarity can regulate the polarity of osteoblasts through the TRPV4 channel. This finding aligns with recent research demonstrating that TRPV4 can impact hepatocellular carcinoma metastasis by regulating single-cell polarity[58]. These findings suggest that the mechanism revealed in our study holds significant importance. Moreover, the involvement of extracellular osmolarity indicates that this mechanism may have widespread implications in various physiological and pathological processes, including organogenesis and cancer metastasis.

In conclusion, this study delved into the intriguing realm of extracellular osmolarity and its impact on osteoblasts. Our findings shed light on the fascinating role of extracellular osmolarity in promoting the migration of osteoblasts. The pivotal players in this phenomenon are the TRPV4 channels, which serve as sensory mechanisms, responding to alterations in extracellular osmolarity. These channels, in turn, influence various cellular components, such as the cytoskeleton structure, FA, and cell polarity, thereby impacting the behavior of osteoblast migration. By elucidating the intricate connection between extracellular osmolarity, TRPV4 channels, and osteoblast migration, our results offer profound insights into the mechanisms underlying bone formation, remodeling, and the treatment of bone diseases. The potency of regulating extracellular osmolarity to enhance osteoblast migration holds significant implications for therapeutic approaches aimed at promoting bone regeneration, as it provides an avenue for targeting the migration aspect of osteoblasts.

Notably, calcium signaling is central to the mechanisms explored in this study. However, it is important to note that calcium signaling impacts many cell functions through a multitude of pathways and signaling molecules, such as integrins and PIEZOs, which could also influence osteoblast behavior. These key proteins were not examined in this study. Future research will be required to delve further into these aspects to provide a more comprehensive understanding of the signaling dynamics involved in osteoblast migration and bone biology.

Methods

Cell lines and cell culture

We obtained MC3T3-E1 from the Central Laboratory of Peking University Third Hospital, cultured in DMEM-high glutamine medium containing 10% fetal bovine serum (Gibco, America), and then grown at 37 °C and 5% CO_2. The cells were subcultured to ~75–90% confluency for most experiments.

Antibodies and drug treatment

Antibodies and drugs	Company
Fetal bovine serum	HyClone, America
Trypsin-EDTA (0.25%)	Yeasen, China
DMEM-high glutamine medium	Gibco, America
Phosphate buffered saline	Gibco, America
Dimethyl sulfoxide(DMSO)	Solarbio, China
TRNzol	TIANGEN, China
RIPA lysis buffer	APPLYGEN, China
Paxillin antibody	Abcam, America
TRPV4 antibody	Abcam, America
GAPDH antibody	CST, America
Rac1/Cdc42 antibody	CST, America
Crystal violet staining solution	Beyotime, China
HRP-labeled goat anti-rabbit IgG	Beyotime, China
HRP-labeled goat anti-mouse IgG	Beyotime, China
Actin-tracker red-rhodamine	Beyotime, China
DAPI staining solution	Beyotime, China
Hoechst 33342	Beyotime, China
Fluo-4 AM	Beyotime, China

Alexa Fluor 594 - conjugated goat anti-mouse IgG	ZSGB-BIO, China
Alexa Fluor 488- conjugated goat anti-rabbit IgG	ZSGB-BIO, China
GSK1016790A	Selleck, America
HC067047	Selleck, America
ML141	MCE, America
NSC23766	MCE, America
Y27632	MCE, America
Fasudil	MCE, America
Annexin V-FITC/PI apoptosis detection Kit	KeyGEN BioTECH, China

Preparation of media with different osmolarities

To obtain media with different osmolarities, sucrose solutions were prepared at concentrations of 180, 300, and 420 mM. DMEM culture medium was supplied with 20% FBS to obtain a complete medium with an osmolarity of about 300 mOsm. Then the complete medium was mixed with the sucrose solutions to obtain media with osmolarities of 240 mOsm (hypotonic medium), 300 mOsm (isotonic medium), and 360 mOsm (hypertonic medium).

Measurement of the intracellular pressure

Intracellular pressure measurements were conducted using the 900 A micropressure system (WPI, America) with the servo-null method according to the manufacturer's instructions. Microelectrodes were fabricated from a glass capillary with dimensions of 0.75 mm inner diameter and 1.0 mm outer diameter using a micropipette puller (PC-100, Narishige, Japan) in one-stage pull mode with settings of Heat 55 V and Weights: 250 g. Before measurement, the microelectrodes were calibrated with a 1 M NaCl solution while the calibration chamber contained a 0.1 M NaCl solution, using a provided calibration chamber and a pressure source. The calibrated microelectrodes were then mounted on a piezo-driven xyz micromanipulator (SN-PCZ-50R, WPI, America) within the MAWORDE workstation (Longfubiotech, China) set at 37 °C with 5% CO_2. Pressure signals were recorded using a four-channel AD converter. The measurement of intracellular pressure of osteoblasts was conducted 15 min after introducing media with different osmolarities and stopped after 15 min of measurement. Interphase osteoblasts were chosen as the target cells, and caution should be taken to avoid inserting the tip into the nucleus. During measuring, the microelectrode tip was inserted into the cells at a 45-degree angle and then gently retracted to alleviate compression on the cells. This position was maintained for at least 5 s, during which the intracellular pressure was determined by calculating the average pressure.

Single-cell trajectory

To track single-cell migration trajectories, MC3T3-E1 cells were seeded in a well plate and cultured overnight to reach a confluence of ~30–40%. The cells were then stained with Hoechst 33342 and placed in a MAWORDE workstation (Longfubiotech, China) equipped with an EVOS FL Auto imaging system (Invitrogen, America). Images were captured every 30 min, and the resulting image series were imported into ImageJ. The Manual Tracking plugin in ImageJ was utilized to obtain the single-cell trajectories.

Wound healing assay

MC3T3-E1 cells were seeded at a density of $(2–4) \times 10^5$ cells/well per group, grown to confluence in 96-well plates (Corning, America), and serum-starved for a minimum of 24 h. Cells were scored using a 96-well scribe and washed twice with phosphate buffer (Gibco, America), medium containing 10% serum for different groups was added, and the cell migration process was recorded by real-time microphotography using the Incucyte Live Cell Analysis System IncuCyte S3 (Sartorius, Germany) to count the relative healing rate of the cells.

Transwell assay

About $(1–2) \times 10^4$ osteoblasts were resuspended in 100 μL of DMEM medium with 10% FBS and were placed in the upper well of 8-μm pore-size transwell 24-insert plates (NEST, America), 500 μL of culture medium of different groups was added to the lower chambers. After 24 h, the cells were fixed with 4% Paraformaldehyde for 30 min, and the cells remaining on the top of the transwell membranes were removed with cotton swabs, the cells migrating through the pores to the lower surface were stained with crystal violet (Beyotime, China). Four to five fields of view were randomly selected, photomicroscopic images were obtained, and the cells in each image were counted using ImageJ.

Cell apoptosis assay

Annexin V-FITC apoptosis detection kit (KeyGEN BioTECH, China) was used to detect the apoptosis rate of MC3T3-E1 cells under the manufacturer's guidelines. The MC3T3-E1 cells were cultivated in 6-well plates (4×10^5 cells/well) for a 24-h period, after which they were subjected to different osmolarity solutions for a further 24 h. The cells were then harvested by trypsinization, washed twice with PBS, and centrifuged at 800×*g* for 5 min. Cells were resuspended in 500 μL of binding buffer and mixed with 5 μL of Annexin V-FITC and 5 μL of propidium iodide (PI). The cells were then immediately analyzed using a flow cytometer (Beckman, USA). CytExpert software was employed for the quantification of cell apoptosis. All experiments were conducted in triplicate and repeated at least three times.

Immunofluorescence staining

MC3T3-E1 cells were inoculated in each group at a density of $(1–2) \times 10^5$ cells/well on glass-bottomed Petri dishes (NEST, China) with a diameter of 20 mm, fixed for 15 min in 4% histiocyte fixative (Solarbio, China), washed three times with PBS, the cells were then treated with Immunostaining Permeabilization Buffer with Saponin (Beyotime, China) for 10 min. Cells were blocked with goat serum (ZSGB-BIO, China) for 1 h at RT, the blocking solution was removed, stained with Anti-Paxillin antibody (1:250, CST, America), incubated overnight at 4 °C, washed three times with PBS, and stained with Alexa Fluor 594 - Conjugated Goat anti-Mouse IgG (1:300, ZSGB-BIO, China) was incubated avoiding light for 1 h. Cells were washed as described above, the microfilament red fluorescent probe Actin-Tracker Red-Rhodamine (1:100, Beyotime, China) was added and incubated for 1 h at RT away from light, and then the nuclei were stained by adding DAPI staining solution (Beyotime, China), and incubated for 10 min at RT away from light. The cells were stored at 4 °C and imaged using a confocal laser scanning microscope (Zeiss, Germany) for cell imaging.

Analysis of stress fiber direction

The line connecting the most distant two points on the cell is identified as the cell's long axis. Stress fibers longer than 20 μm were selected, and the angles between these stress fibers and the long axis were measured using ImageJ.

Calcium imaging

The experiment employed the Fluo-4 AMcalcium ion fluorescent probe to monitor dynamic changes in intracellular free calcium ion concentration. First, dilute Fluo-4 AM in PBS buffer to a working concentration of 2 μM. Then, remove the cell culture medium and wash the cells three times with prewarmed PBS buffer. Add enough Fluo-4 AM working solution to completely cover the cell layer and incubate the cells at 37 °C with 5% CO_2 for 20 min. After incubation, wash the cells three additional times with PBS buffer and observe the fluorescence using a fluorescence microscope.

Protein extraction and western blot analysis

RIPA lysis buffer (APPLYGEN, China) and Protease inhibitor cocktail (APPLYGEN, China) in the ratio of 100:1 were added according to the number of cells, lysed in an ice bath, and centrifuged at 12,000 r/min at 4 °C for 15 min. The supernatant was collected and

the total protein was quantified using the BCA Protein Assay Kit (APPLYGEN, China), 5× SDS-PAGE protein Loading Buffer (Yeasen, China) was added, and the protein was denatured sufficiently by the metal bath at 100 °C for 5 min. The protein samples were transferred from 8 to 12% gel to PVDF membrane, closed with 5% skimmed milk, and added GAPDH Antibody (CST, America) and TRPV4 Antibody (Abcam, America) respectively, and incubated at 4 °C overnight. The membrane was washed three times with TBST (APPLYGEN, China), and HRP-labeled goat anti-rabbit IgG, HRP-labeled goat anti-mouse IgG (Beyotime, China) were added respectively, and incubated for 1 h at RT. After washing the membrane three times with TBST, Super ECL Detection Reagent (Yeasen, China) was added to the membrane and the intensity of the bands was detected using Tanon 5200 Multi (Tanon, China). Protein expression was quantified using ImageJ software.

RNA isolation and quantitative real-time PCR

Total mRNA was extracted using TRNzol Universal Reagent (TIANGEN, China) according to the manufacturer's protocol, and the concentration and purity of RNA were determined using NanoDrop OneC (Thermo Fisher, America). Then, 2 μg of RNA was converted into complementary DNA using the Hifair II 1st Strand cDNA Synthesis Kit (Yeasen, China). Template, primers, and Hieff qPCR SYBR Green Master Mix were added to the amplification system, and the qRT-PCR reaction was performed on Quantstudio 5 (Thermo Fisher, America). Relative gene expression was calculated using a $2^{-\Delta\Delta Ct}$ method by normalization with GAPDH. Primer sequences:

Genes (Mouse)	Forward	Reverse
TRPV4	5'-ATGGCAGATCC TGGTGATGG-3'	5'-GGAACTTCATA CGCAGGTTTGG-3'
Cdc42	5'-GCAGTTACGGT TATGATTGG-3'	5'-TGATGGGTTTC TGTTTGTTC-3'
Rac1	5'-GAGACGGAGCT GTTGGTAAAA-3'	5'-ATAGGCCCAGA TTCACTGGTT-3'
GAPDH	5'-GGGAGCCAAAAG GGTCATCATCTC-3'	5'-CCATGCCAGTG AGCTTCCCGTTC-3'

Statistics and reproducibility

Statistical analyses were performed using IBM SPSS Statistics 27. Statistical significance was assessed by unpaired *t*-test, one-way ANOVA followed by Tukey's test, two-way ANOVA test, or two-way ANOVA followed by Tukey's test where appropriate. Significance levels were set to $P = 0.05$. Sample sizes were determined based on prior protocols and ensured statistical significance. Migration speed was analyzed in over 60 cells. Wound healing, Transwell, apoptosis, Western blot, and PCR assays had at least three replicates. Intracellular pressure, calcium fluorescence, aspect ratio, and FA number were measured in at least 20 cells per condition. Stress fiber orientation was assessed in five cells per group.

Reporting summary

Further information on research design is available in the Nature Portfolio Reporting Summary linked to this article.

Data availability

The source data underlying the graphs presented in this paper are available in Supplementary Data. Uncropped and unedited blot images are displayed in Supplementary Fig. 5. All additional data were included within the figures and Supplementary Figs.

Received: 26 September 2024; Accepted: 17 March 2025;
Published online: 29 March 2025

References

1. Dirckx, N., Moorer, M. C., Clemens, T. L. & Riddle, R. C. The role of osteoblasts in energy homeostasis. *Nat. Rev. Endocrinol.* **15**, 651–665 (2019).
2. Lee, W. C., Guntur, A. R., Long, F. & Rosen, C. J. Energy metabolism of the osteoblast: implications for osteoporosis. *Endocr. Rev.* **38**, 255–266 (2017).
3. Thiel, A. et al. Osteoblast migration in vertebrate bone. *Biol. Rev. Camb. Philos. Soc.* **93**, 350–363 (2018).
4. Su, P. et al. Mesenchymal stem cell migration during bone formation and bone diseases therapy. *Int. J. Mol. Sci*. https://doi.org/10.3390/ijms19082343 (2018).
5. Feng, X. & McDonald, J. M. Disorders of bone remodeling. *Annu. Rev. Pathol.* **6**, 121–145 (2011).
6. Chen, J. -H., Liu, C., You, L. & Simmons, C. A. Boning up on Wolff's Law: mechanical regulation of the cells that make and maintain bone. *J. Biomech.* **43**, 108–118 (2010).
7. Carina, V. et al. Bone's response to mechanical loading in aging and osteoporosis: molecular mechanisms. *Calcif. Tissue Int.* **107**, 301–318 (2020).
8. Gao, Y. et al. Migration and differentiation of osteoclast precursors under gradient fluid shear stress. *Biomech. Model. Mechanobiol.* **18**, 1731–1744 (2019).
9. Refaaq, F. M., Chen, X. & Pang, S. W. Effects of topographical guidance cues on osteoblast cell migration. *Sci. Rep.* **10**, (2020). 20003.
10. Takemoto, F., Uchida-Fukuhara, Y., Kamioka, H., Okamura, H. & Ikegame, M. Mechanical stretching determines the orientation of osteoblast migration and cell division. *Anat. Sci. Int.* **98**, 521–528 (2023).
11. Seetharaman, S. & Etienne-Manneville, S. Cytoskeletal crosstalk in cell migration. *Trends Cell Biol.* **30**, 720–735 (2020).
12. Ridley, A. J. et al. Cell migration: integrating signals from front to back. *Science* **302**, 1704–1709 (2003).
13. Dias Gomes, M. & Iden, S. Orchestration of tissue-scale mechanics and fate decisions by polarity signalling. *EMBO J.* **40**, e106787 (2021).
14. Houk, A. R. et al. Membrane tension maintains cell polarity by confining signals to the leading edge during neutrophil migration. *Cell* **148**, 175–188 (2012).
15. Lo, C. M., Wang, H. B., Dembo, M. & Wang, Y. L. Cell movement is guided by the rigidity of the substrate. *Biophys. J.* **79**, 144–152 (2000).
16. Jungbauer, S., Gao, H., Spatz, J. P. & Kemkemer, R. Two characteristic regimes in frequency-dependent dynamic reorientation of fibroblasts on cyclically stretched substrates. *Biophys. J.* **95**, 3470–3478 (2008).
17. Goehring, N. W. & Grill, S. W. Cell polarity: mechanochemical patterning. *Trends Cell Biol.* **23**, 72–80 (2013).
18. Fritton, S. P. & Weinbaum, S. Fluid and solute transport in bone: flow-induced mechanotransduction. *Annu. Rev. Fluid Mech.* **41**, 347–374 (2009).
19. Tao, J., Li, Y., Vig, D. K. & Sun, S. X. Cell mechanics: a dialogue. *Rep. Prog. Phys.* **80**, 036601 (2017).
20. Chengappa, P., Sao, K., Jones, T. M. & Petrie, R. J. Intracellular pressure: a driver of cell morphology and movement. *Int. Rev. Cell Mol. Biol.* **337**, 185–211 (2018).
21. Petrie, R. J., Koo, H. & Yamada, K. M. Generation of compartmentalized pressure by a nuclear piston governs cell motility in a 3D matrix. *Science* **345**, 1062–1065 (2014).
22. Stroka, K. M. et al. Water permeation drives tumor cell migration in confined microenvironments. *Cell* **157**, 611–623 (2014).
23. SenGupta, S., Parent, C. A. & Bear, J. E. The principles of directed cell migration. *Nat. Rev. Mol. Cell Biol.* **22**, 529–547 (2021).

24. Sun, M. & Zaman, M. H. Modeling, signaling and cytoskeleton dynamics: integrated modeling-experimental frameworks in cell migration. *Wiley Interdiscip. Rev. Syst. Biol. Med*. https://doi.org/10.1002/wsbm.1365 (2017).
25. Elkhatib, N. et al. Fascin plays a role in stress fiber organization and focal adhesion disassembly. *Curr. Biol.* **24**, 1492–1499 (2014).
26. Roffay, C. et al. Passive coupling of membrane tension and cell volume during active response of cells to osmosis. *Proc. Natl. Acad. Sci. USA* https://doi.org/10.1073/pnas.2103228118 (2021).
27. Ajubi, N. E., Klein-Nulend, J., Alblas, M. J., Burger, E. H. & Nijweide, P. J. Signal transduction pathways involved in fluid flow-induced PGE2 production by cultured osteocytes. *Am. J. Physiol.* **276**, E171–E178 (1999).
28. Hu, M. et al. Mechanobiological modulation of in situ and in vivo osteocyte calcium oscillation by acoustic radiation force. *Ann. N. Y. Acad. Sci.* **1460**, 68–76 (2020).
29. Endesh, N. et al. Independent endothelial functions of PIEZO1 and TRPV4 in hepatic portal vein and predominance of PIEZO1 in mechanical and osmotic stress. *Liver Int.* **43**, 2026–2038 (2023).
30. Peana, D., Polo-Parada, L. & Domeier, T. L. Arrhythmogenesis in the aged heart following ischaemia-reperfusion: role of transient receptor potential vanilloid 4. *Cardiovasc. Res.* **118**, 1126–1137 (2022).
31. Lee, H. P., Stowers, R. & Chaudhuri, O. Volume expansion and TRPV4 activation regulate stem cell fate in three-dimensional microenvironments. *Nat. Commun.* **10**, 529 (2019).
32. Li, X. et al. Calcium and TRPV4 promote metastasis by regulating cytoskeleton through the RhoA/ROCK1 pathway in endometrial cancer. *Cell Death Dis.* **11**, 1009 (2020).
33. Kwon, D. H. et al. TRPV4-Rho GTPase complex structures reveal mechanisms of gating and disease. *Nat. Commun.* **14**, 3732 (2023).
34. Kim, M. K., Ramachandran, R. & Séguin, C. A. Spatiotemporal and functional characterisation of transient receptor potential vanilloid 4 (TRPV4) in the murine intervertebral disc. *Eur. Cell Mater.* **41**, 194–203 (2021).
35. Chaker, D. et al. Inhibition of the RhoGTPase Cdc42 by ML141 enhances hepatocyte differentiation from human adipose-derived mesenchymal stem cells via the Wnt5a/PI3K/miR-122 pathway: impact of the age of the donor. *Stem Cell Res. Ther.* **9**, 167 (2018).
36. Song, S. J. et al. Inhibition of Rac1 GTPase activity affects porcine oocyte maturation and early embryo development. *Sci. Rep.* **6**, 34415 (2016).
37. Xue, Z. W. et al. Rho-associated coiled kinase inhibitor Y-27632 promotes neuronal-like differentiation of adult human adipose tissue-derived stem cells. *Chin. Med. J.* **125**, 3332–3335 (2012).
38. Wang, D. et al. The interactions between mTOR and NF-κB: A novel mechanism mediating mechanical stretch-stimulated osteoblast differentiation. *J. Cell Physiol.* https://doi.org/10.1002/jcp.30184 (2020).
39. Yao, W., Gong, Y., Zhao, B. & Li, R. Combined effects of cyclic stretch and TNF-α on the osteogenic differentiation in MC3T3-E1 cells. *Arch. Oral. Biol.* **130**, 105222 (2021).
40. Zhao, Y. et al. Notch signaling and fluid shear stress in regulating osteogenic differentiation. *Front. Bioeng. Biotechnol.* **10**, 1007430 (2022).
41. Wang, X. et al. Fluid shear stress regulates osteoblast proliferation and apoptosis via the lncRNA TUG1/miR-34a/FGFR1 axis. *J. Cell Mol. Med.* **25**, 8734–8747 (2021).
42. Hinton, P. V., Genoud, K. J., Early, J. O., O'Brien, F. J. & Kennedy, O. D. Impact of fluid flow shear stress on osteoblast differentiation and cross-talk with articular chondrocytes. *Int. J. Mol. Sci*. https://doi.org/10.3390/ijms23169505 (2022).
43. Zhang, T. et al. Effect of matrix stiffness on osteoblast functionalization. *Cell Prolif*. https://doi.org/10.1111/cpr.12338 (2017).
44. Aryaei, A., Jayatissa, A. H. & Jayasuriya, A. C. The effect of graphene substrate on osteoblast cell adhesion and proliferation. *J. Biomed. Mater Res. A* **102**, 3282–3290 (2014).
45. Whited, B. M., Whitney, J. R., Hofmann, M. C., Xu, Y. & Rylander, M. N. Pre-osteoblast infiltration and differentiation in highly porous apatite-coated PLLA electrospun scaffolds. *Biomaterials* **32**, 2294–2304 (2011).
46. Danziger, J. & Zeidel, M. L. Osmotic homeostasis. *Clin. J. Am. Soc. Nephrol.* **10**, 852–862 (2015).
47. Wang, M., Yang, Y., Han, L., Xu, F. & Li, F. Cell mechanical microenvironment for cell volume regulation. *J. Cell Physiol.* **235**, 4070–4081 (2020).
48. Cowin, S. C. & Cardoso, L. Blood and interstitial flow in the hierarchical pore space architecture of bone tissue. *J. Biomech.* **48**, 842–854 (2015).
49. Schindeler, A., McDonald, M. M., Bokko, P. & Little, D. G. Bone remodeling during fracture repair: the cellular picture. *Semin. Cell Dev. Biol.* **19**, 459–466 (2008).
50. Einhorn, T. A. & Gerstenfeld, L. C. Fracture healing: mechanisms and interventions. *Nat. Rev. Rheumatol.* **11**, 45–54 (2015).
51. Guilak, F., Leddy, H. A. & Liedtke, W. Transient receptor potential vanilloid 4: the sixth sense of the musculoskeletal system. *Ann. N. Y. Acad. Sci.* **1192**, 404–409 (2010).
52. Yoneda, M. et al. PIEZO1 and TRPV4, which are distinct mechano-sensors in the osteoblastic MC3T3-E1 cells, modify cell-proliferation. *Int. J. Mol. Sci*. https://doi.org/10.3390/ijms20194960 (2019).
53. Goswami, C., Kuhn, J., Heppenstall, P. & Hucho, T. Importance of non-selective cation channel TRPV4 interaction with cytoskeleton and their reciprocal regulations in cultured cells. *PLoS ONE* https://doi.org/10.1371/journal.pone.0011654 (2010).
54. Huang, S. et al. TRPV4 promotes metastasis in melanoma by regulating cell motility through cytoskeletal rearrangement. *Int. J. Mol. Sci*. https://doi.org/10.3390/ijms232315155 (2022).
55. Gilchrist, C. L. et al. TRPV4-mediated calcium signaling in mesenchymal stem cells regulates aligned collagen matrix formation and vinculin tension. *Proc. Natl Acad. Sci. USA* **116**, 1992–1997 (2019).
56. Costa, P., Blowes, L. M., Laly, A. C. & Connelly, J. T. Regulation of collective cell polarity and migration using dynamically adhesive micropatterned substrates. *Acta Biomater.* **126**, 291–300 (2021).
57. Fischer, R. S. et al. Contractility, focal adhesion orientation, and stress fiber orientation drive cancer cell polarity and migration along wavy ECM substrates. *Proc. Natl. Acad. Sci. USA* https://doi.org/10.1073/pnas.2021135118 (2021).
58. Liu, J. et al. Inhibition of TRPV4 remodels single cell polarity and suppresses the metastasis of hepatocellular carcinoma. *Cell Death Dis.* **14**, 379 (2023).

Acknowledgements

This work has been supported by the National Natural Science Foundation of China, Grant numbers: 82272597, 82072538, 12232019, and 12272388.

Author contributions

X.W., L.L., and M.Z. discussed and conceptualized the study. X.W., Y.L., and Y.Y. designed the experiments, Y.L. and X.W. performed most of the experiments. X.W., Y.L., Y.Y., and M.H. analyzed the data. X.W., Y.Y., and Y.L. wrote the original manuscript. X.W., L.L., and M.Z. edited and revised the manuscript. All authors discussed the results and commented on the manuscript.

Competing interests

The authors declare no competing interests.

Additional information

Supplementary information The online version contains supplementary material available at https://doi.org/10.1038/s42003-025-07946-8.

Correspondence and requests for materials should be addressed to Xiaohuan Wang, Long Li or Mouwang Zhou.

Peer review information *Communications Biology* thanks the anonymous reviewers for their contribution to the peer review of this work. Primary Handling Editors: Martina Rauner and Joao Valente. A peer review file is available.